International Hormesis Society
w w w . H o r m e s i s S o c i e t y . o r g

PROTECTIVE BYSTANDER EFFECTS SIMULATED WITH THE STATE-VECTOR MODEL

Helmut Schöllnberger □ Department of Materials Engineering and Physics, Division of Physics and Biophysics, University of Salzburg, Hellbrunnerstr. 34, A-5020 Salzburg, Austria

Peter M. Eckl □ Department of Cell Biology, University of Salzburg, Hellbrunnerstr. 34, A-5020 Salzburg, Austria

□ Apoptosis induced in non-hit bystander cells is an important biological mechanism which operates after exposure to low doses of low-LET radiation. This process was implemented into a deterministic multistage model for *in vitro* neoplastic transformation: the State-Vector Model (SVM). The new model is tested on two data sets that show a reduction of the transformation frequency below the spontaneous level after exposure of the human hybrid cell line CGL1 to low doses of γ-radiation. Stronger protective effects are visible in the data for delayed plating while the data for immediate plating show more of an LNT-like dose-response curve. It is shown that the model can describe both data sets. The calculation of the time-dependent numerical solution of the model also allows to obtain information about the time-dependence of the protective apoptosis-mediated process after low dose exposures. These findings are compared with experimental observations after high dose exposures.

Keywords: low dose, bystander effect, LNT, U-shaped, apoptosis, neoplastic transformation

INTRODUCTION

Extensive efforts have been devoted to apply biomathematical models to investigate biological effects of ionizing radiation (Little 1995; Luebeck *et al.* 1999; Brenner *et al.* 2001; Nikjoo and Khvostunov 2003; Scott 2004; Schöllnberger *et al.* 2004, 2005, 2006). Such studies can be especially valuable in areas where it is still unclear which biological effects are the rate limiting mechanisms. Low dose exposure conditions represent such an area. Mathematical models allow to include different effects such as cellular defense mechanisms (Feinendegen and Pollycove 2001) and bystander effects which can be detrimental (Sawant *et al.* 2001; Morgan 2003a, 2003b; Belyakov *et al.* 2005) and protective (Barcellos-Hoff and Brooks 2001; Iyer and Lehnert 2002; Belyakov *et al.* 2005; Jürgensmeier *et al.* 1994a). The most recent reviews of bystander effects and related topics are by Barcellos-Hoff and Costes (2006), Chaudhry (2006), Brooks (2005),

Address correspondence to Helmut Schöllnberger, PhD, Department of Materials Engineering and Physics, Division of Physics and Biophysics, University of Salzburg, Hellbrunnerstr. 34, A-5020 Salzburg, Austria. Voice: +43 662 8044 5709; fax: +43 662 8044 150; E-mail: helmut.schoellnberger@sbg.ac.at.

Mothersill and Seymour (2005, 2006) and Prise et al. (2005). These effects can be regulated during model simulations and data fitting. When the models are tested on data sets it is possible to gain an understanding which mechanisms might operate in the cells and between them to produce the data at hand. Ideally, the models can be used to predict new effects and, for low dose exposures, the form of dose-response relationships.

Recent years brought fascinating discoveries in this field such as adaptive responses measured by a *single low dose* of low-LET radiations that induce neoplastic transformation frequencies significantly *below* those induced spontaneously (Azzam *et al.* 1996; Redpath and Antoniono 1998; Redpath *et al.* 2001, 2003). The cell culture study by Azzam *et al.* (1996) was the first to show this *in vitro* effect of low doses of γ-radiation up to 100 mGy, a dose approximately 100 times larger than the yearly dose from environmental background low-LET radiation in the U.S. A dose of 100 mGy caused a statistically significant lower neoplastic transformation frequency per surviving cell (TFSC) than the spontaneous TFSC at 0 dose (Azzam *et al.* 1996). On the other hand manifold studies showed detrimental bystander effects (Nagasawa and Little 1999, 2002; Zhou *et al.* 2000; Morgan 2003a, 2003b). Such supralinear behavior typically means that the actual dose-response curve at low doses lies above a linear extrapolation from a higher dose to the origin. This paper describes how a protective apoptosis-mediated process (Jürgensmeier et al. 1994a, 1994b, Bauer 1996, Bauer 2000, Portess et al. 2007) is included into a biomathematical model for *in vitro* neoplastic transformation. The latter is an important biological endpoint that has been extensively investigated to assess the biological effects after radiation exposures (Little 1985, Hall and Hei 1985, Miller et al. 1979, 1995). The model is then tested on an important and representative data set (Redpath et al. 2001) that shows protective effects against neoplastic transformation after exposure of the nontumorigenic HeLa × skin fibroblast cell line CGL1 to low doses of γ-radiation.

The terms "detrimental" and "protective" as used in the current study refer to the endpoints analyzed here and not necessarily to carcinogenesis in humans. When we refer to *protective* effects seen in the transformation studies of Redpath et al. (2001), the limitations of *in vitro* cell transformation measurements need to be borne in mind when interpreting data for the purposes of radiological protection criteria (Mill et al. 1998). While it has been stated that the data for neoplastic transformation have uncertain implications for the question of the LNT model (NCRP 2001), other researchers point out the importance of this endpoint. Dr. R.E.J. Mitchel (personal communication) argues that if a cell *in vivo* is "near transformation" for whatever reason and would eventually develop into a cancer, and if radiation protects against and slows/reverses that process as demonstrated by Mitchel et al. (1999, 2002, 2003, 2004) and Mitchel (2006, 2007), that this would be critically important. With respect to bystander

effects it is noted that when we here refer to detrimental aspects of this effect, it should be remembered that it is not yet clear whether at low doses bystander effects are predominately detrimental or protective with respect to cancer induction in humans (Belyakov et al. 2005).

MATERIALS AND METHODS

The Model

Fig. 1 shows a conceptual view of the State-Vector Model (SVM) (Crawford-Brown and Hofmann 1990). Differential equations can be derived from this scheme and are given in equations (1)-(6). A state vector denotes the fraction of cells in each of the states at time *t*:

$$\left[\frac{N_0(t)}{N_T(t)} , \frac{N_{1s}(t)}{N_T(t)} , \frac{N_{1ns}(t)}{N_T(t)} , \frac{N_2(t)}{N_T(t)} , \frac{N_3(t)}{N_T(t)} , \frac{N_4(t)}{N_T(t)} \right].$$

Here, $N_i(t)$ is the number of cells in state i at time t. It is $N_T(t) = N_0(t) + N_{1s}(t) + N_{1ns}(t) + N_2(t) + N_3(t) + N_4(t)$.
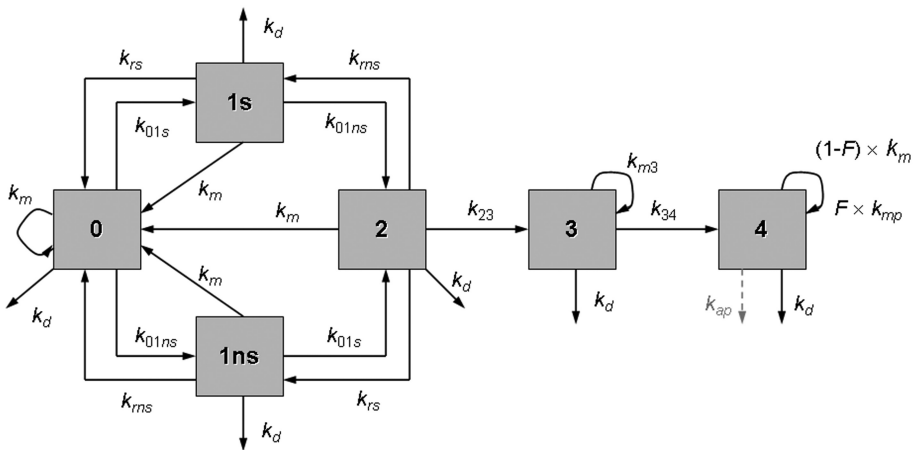

FIGURE 1: Pictorial representation of the State-Vector Model. Cells in state 0 represent normal cells. The rate constants of DSB formation in specific transcriptionally active areas of the genome and in other inactive domains of DNA are denoted as k_{01s} and k_{01ns}, respectively. k_{23} denotes the rate constant of DSB interaction and k_{34} is the rate constant of damage fixation. State 4 cells are initiated and can be eliminated by a dose-rate independent protective apoptosis-mediated bystander effect (k_{ap}, dashed arrow) in addition to the dose-rate dependent pathway for necrotic cell killing (k_d). The mitotic rate constant is denoted as k_m (cell divisions per day). A fraction *F* of the initiated cells cycles at an elevated mitotic rate (k_{mp}). The rate constants for repair of DSBs in transcriptionally active and inactive DNA are represented by k_{rs} and k_{rns}, respectively. Cell-cycle associated postreplication repair (rate constant k_m) is possible for cells in states 1s, 1ns, and 2.

$$\frac{dN_0}{dt} = (k_m - k_{01s} - k_{01ns} - k_d) N_0 + (k_{rs} + 2k_m) N_{1s} +$$
$$(k_{rns} + 2k_m) N_{1ns} + (k_{rs} + 2k_m) N_2 \tag{1}$$

$$\frac{dN_{1s}}{dt} = k_{01s} N_0 + k_{rns} N_2 - (k_{01ns} + k_{rs} + k_m + k_d) N_{1s} \tag{2}$$

$$\frac{dN_{1ns}}{dt} = k_{01ns} N_0 + k_{rs} N_2 - (k_{01s} + k_{rns} + k_m + k_d) N_{1ns} \tag{3}$$

$$\frac{dN_2}{dt} = k_{01ns} N_{1s} + k_{01s} N_{1ns} - (k_{rs} + k_{rns} + k_{23} + k_m + k_d) N_2 \tag{4}$$

$$\frac{dN_3}{dt} = k_{23} N_2 + (k_{m3} - k_{34} - k_d) N_3 \tag{5}$$

$$\frac{dN_4}{dt} = k_{34} N_3 + (F k_{mp} + (1 - F) k_m - k_d) N_4 \tag{6}$$

The rate constants k_{ij} (unit of time^{-1}) denote transitions from state i to state j. The model describes a series of background (endogenous) and radiation induced events in the formation of *in vitro* neoplastic transformation. State 0 cells represent normal CGL1 cells. Cells in states 1s and 1ns contain a double strand break (DSB) in transcriptionally active and inactive DNA, respectively. The rate constants of DSB formation contain a background component (subscript *b*) that describes the formation of DSBs by endogenous influences and a radiation-induced component (subscript *r*): $k_{01s} = k_{01sb} + k_{01sr} \times DR$ and $k_{01ns} = k_{01nsb} + k_{01nsr} \times DR$. Here, DR denotes the dose rate. Cells in state 2 contain both types of DSBs. The DSB repair pathways include a cell cycle independent contribution and a cell cycle associated contribution. Quiescent cells in state 1s can undergo repair with rate constant k_{rs}. Quiescent state 1ns cells can be repaired with rate constant k_{rns}. In the SVM DSB repair with a rate governed by the mitotic rate constant k_m is allowed for cells in states 1s, 1ns and 2 (Fig. 1). It is emphasized that despite its relation to k_m this repair mechanism is not active during mitosis but correlates with it, i.e. the higher the mitotic rate the higher the number of cells undergoing postreplication repair. All three repair mechanisms (k_{rs}, k_{rns}, and the cell cycle associated postreplication repair) represent homologous recombination (HR) and non-homologous end-joining (NHEJ). Each cell cycle associated repair produces two undamaged cells in state 0 (refer to eq. (1)).

The two DSBs in state 2 cells can interact with each other with rate constant k_{23} ($k_{23} = k_{23r} \times (DR_b + DR)$) and form chromosome aberrations such as translocations. Here, DR_b denotes the dose rate from environmental background radiation. It was assumed that $DR_b = 1$ mGy/yr. State

4 cells are said to be initiated and can no longer be repaired. The genomic damage is made permanent when state 3 cells undergo mitosis with rate constant $k_{m3} = (1 - P_4) \times k_m$. Rate constant $k_{34} = P_4 \times k_m$. Here, P_4 denotes the probability per cell division that a state 3 cell develops into an unrepairable state 4 cell (Crawford-Brown and Hofmann 1990: $P_4 = 5 \cdot 10^{-4}$). A fraction F of the initiated cells can acquire a growth advantage (often referred to as "promotion") after contact inhibition has been lost for these cells. They divide with an enhanced mitotic rate constant $k_{mp} = k_{mmult} \times k_m$ (Fleishman et al., submitted). This fraction can be calculated as the probability that 4, 5 or 6 dead cells are surrounding an initiated cell. It is assumed that then contact inhibition is lost (Crawford-Brown and Hofmann 1990). Cells in states 0, 1s, 1ns, 2, 3 and 4 can die with rate constant k_d ($k_d = k_{db} + k_{dr} \times DR$).

Many values of rate constants and parameters in the SVM can be taken from the literature such as $k_{rs} = 80$ day^{-1} (Mebust et al. 2002) and $k_{rns} = 3.12$ day^{-1} (Crawford-Brown and Hofmann 1990). Experimental evidence supports the use of a larger rate constant for the DSB repair in transcriptionally active DNA, compared to the repair in inactive DNA (Sak and Stuschke 1998, Broome et al. 1999). For CGL1 cells $k_m = 1.2$ day^{-1} (Mendonca et al. 1989; corresponding to a doubling time of 20 hours during exposure, the one day holding period and exponential growth), $k_m = 0.026$ day^{-1} during confluent growth with $k_{db} = 0$. This value for k_m is based on an analysis of the growth curve for CGL1 cells given in Mendonca et al. (1989). Based on earlier findings (Crawford-Brown and Hofmann 1990), the approximation $k_{01s} = 0$ is used and $k_{23r} = 1$ Gy^{-1}. After approximately 10 days the cultures become confluent (Mendonca et al. 1989). For immediate plating the simulation ends at 25 + ET days where ET is the exposure time at the different doses (delayed plating: 26 days + ET). Survival data revealed that up to 1 Gy no significant cell killing occurred (personal communication Dr. J. Leslie Redpath). Therefore, k_{dr} = 0. In all model fits and simulations of the Redpath *et al.* (2001) data F = 1 was used because the fraction of cells that has lost contact inhibition is 1, i.e. in all CGL1 cells there is no contact inhibition: they do not respond to contact inhibition signals and continue to divide (Stanbridge and Wilkinson 1978). Other cell lines, including C3H 10T1/2 cells, show contact inhibition when they enter plateau phase. Because no fraction of the CGL1 cells cycle at an elevated mitotic rate, k_{mmult} was set to 1.

The data

The data by Redpath *et al.* (2001) show the TFSC versus absorbed dose in CGL1 cells irradiated with γ-rays (1 mGy to 1 Gy; the low doses were delivered at DR = 3.3 mGy/min). The data for delayed plating show a stronger protective effect (a reduction of the TFSC *below* the control

level) than the data for immediate plating (Redpath *et al.* 2001). To fit these data we calculate for each dose

$$f_4(t_{\text{end}}) = \frac{N_4(t_{end})}{N_0(t_{end}) + N_{1s}(t_{end}) + N_{1ns}(t_{end}) + N_2(t_{end}) + N_3(t_{end}) + N_4(t_{end})}, \quad (7)$$

with t_{end} = time point at the end of the experiment.

Apoptosis-mediated protective bystander effects

A series of well designed experiments (Höfler et al. 1993, Jürgensmeier et al. 1994a, 1994b, Langer et al. 1996, Eckert and Bauer 1998, Dormann and Bauer 1998, Dormann et al. 1999, Heigold et al. 2002; reviewed by Bauer 1996, 2000) showed that apoptosis can be induced in transformed cells via neighboring healthy cells. In an experimental tissue culture system the addition of exogenous TGF-β is required for maximal intercellular induction of apoptosis, but transformed cell-derived TGF-β is sufficient for induction of intercellular signaling (Bauer 2000). Two main pathways for the intercellular signaling between nontransformed and transformed fibroblasts have been identified: the hypochlorous acid/hydroxyl radical pathway (Fig. 2) and the NO/peroxynitrite pathway (Bauer 2000). Transformed cells release TGF-β
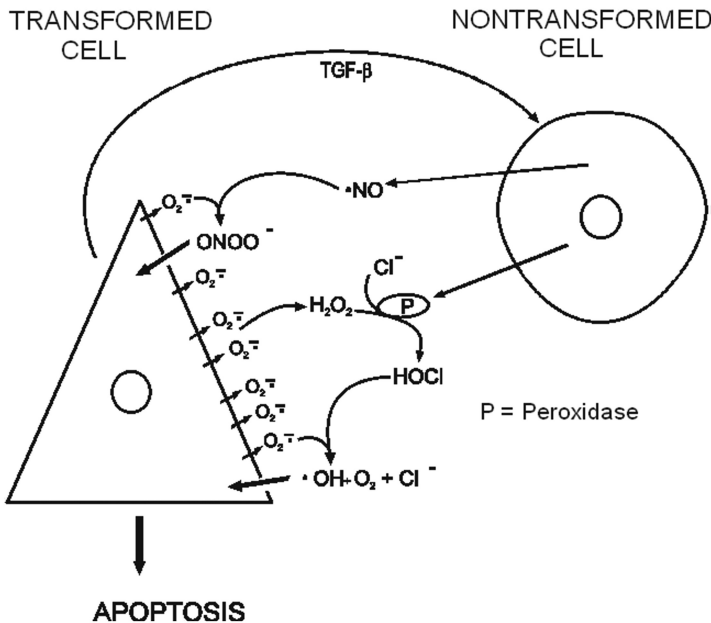

FIGURE 2: HOCl/hydroxyl radical and NO/peroxynitrite pathways as described by Bauer (2000). Refer to *Materials and Methods* section for details. Figure kindly provided by Dr. G. Bauer.

and generate superoxide anions ($O_2^{\bullet-}$). TGF-β causes the release of peroxidase (a haem enzyme that catalyses the reduction of hydrogen peroxide) from normal cells. Superoxide anions from transformed cells spontaneously dismutate and form hydrogen peroxide (H_2O_2). The latter is used by the peroxidase together with chloride ions, which are present abundantly in biological fluids, to form hypochlorous acid (HOCl). HOCl interacts with superoxide anions to form hydroxyl radicals (•OH), which act as the ultimate apoptosis inducer. Because the range of action of $O_2^{\bullet-}$ is very small, the interaction of $O_2^{\bullet-}$ with HOCl is limited to the vicinity of the transformed cells and thus biases the selective apoptosis induction toward transformed cells only (Bauer 2000). The NO/peroxynitrite pathway is less complicated and is also depicted in Fig. 2.

Experimental evidence also indicates that protective apoptosis-mediated [termed PAM by Scott et al. (2003)] effects can be induced by low-dose low- and high-LET radiation in non-hit bystander cells, whereby neoplastically transformed mammalian cells are eliminated by their non-transformed neighboring cells via intercellular, TGF-β mediated, induction of apoptosis (Portess et al. 2007). For brevity, the PAM process is here referred to as PAM. Evidence that bystander induced cell death can occur by apoptosis has been presented (Mothersill and Seymour 1997) and has been deepened over the years (Lyng et al. 2000, 2002a, 2002b, 2006; Maguire et al. 2005, Konopacka and Rzeszowska-Wolny 2006). A notable new development started with the use of microbeam irradiation of individual cells within explant outgrowth under *in vivo*-like conditions (Belyakov et al. 2002, 2003, 2005). These experiments further established apoptosis as a protective bystander-induced mechanism together with cell differentiation. Scott et al. (2003, 2004) and Scott (2004) have extensively reviewed aspects of apoptosis as a protective bystander effect.

To fit the data, a protective apoptosis mediated bystander effect was built into the model via rate constant k_{ap} (Fig. 1). The parameter k_{ap} governs the rate of commitment of initiated cells in state 4 to bystander-induced apoptosis. The unit for k_{ap} is time^{-1}. The following assumptions are made with respect to the occurrence of this bystander effect (Schöllnberger et al., submitted):

1. PAM is effective at low doses only—no effect at doses ≥ 200 mGy
2. PAM can eliminate cells in state 4 (initiated)
3. $k_{ap} = 0$ at $D = 0$
4. PAM is activated by a dose of 1 mGy of low-LET radiation (based on the data by Azzam *et al.* (1996) and Redpath *et al.* (2001), (2003)) but becomes effective only after the exposure (Portess et al. 2007).
5. PAM is activated for various times after irradiation.

The Redpath *et al.* (2001) data show the transition between protection and detriment between 100 and 300 mGy (Fig. 3). Therefore, PAM
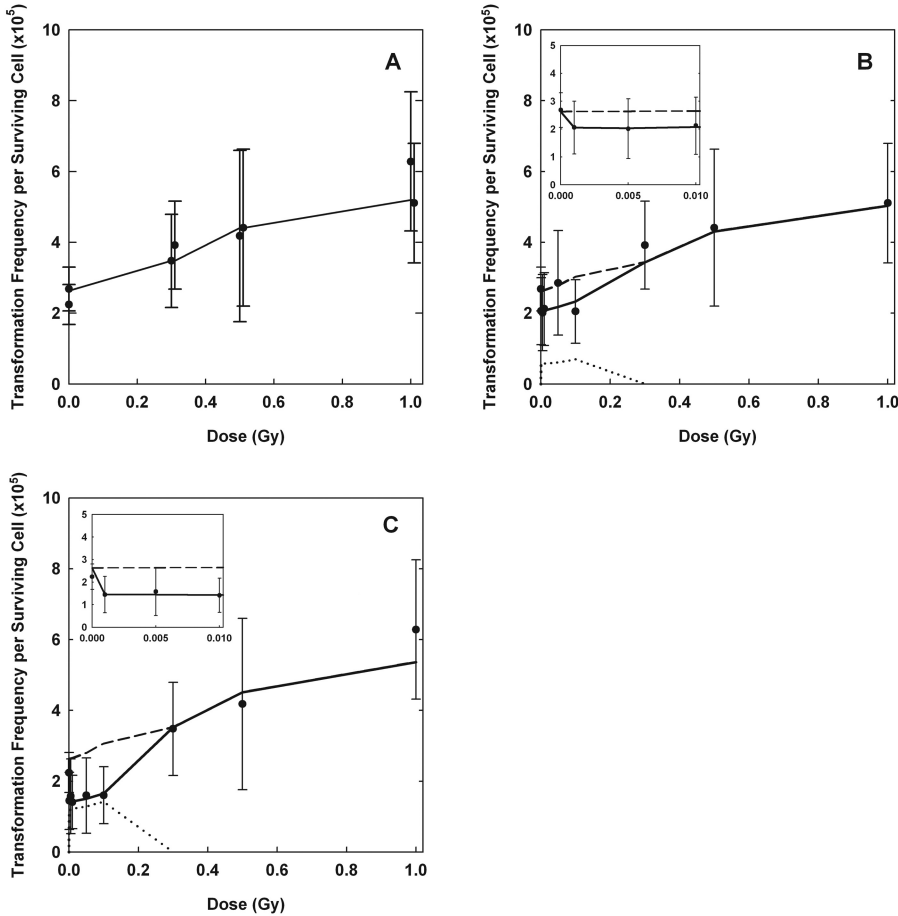
FIGURE 3: TFSC versus dose for CGL1 cells irradiated with γ-radiation (Redpath *et al.* 2001). Error bars represent 95% confidence intervals. Panel A: control and high dose data for immediate and delayed plating and fit of the SVM without the protective apoptosis-mediated bystander effect (fit1). Panel B: data for immediate plating and SVM fit showing the three different contributions (– – – direct, ···· bystander, —— total (fit2)). The direct contribution stems from a forward simulation of the model without PAM with parameter values from fit1. The contribution of the bystanders was calculated as the difference between the forward simulation and fit2. Panel C: data for delayed plating and SVM fit showing the three different contributions (– – – direct, ···· bystander, —— total (fit3)). The inserts show the low-dose range with the x-axis units in Gy.

was switched off (i.e. $k_{ap} = 0$) in the model fits at doses ≥ 200 mGy. Rate constant k_{ap} is currently modeled as dose-rate independent analogous to Scott et al. (2003) and Scott (2004).

The model equations were numerically solved with a stiff solver ("ode15s"*) of the Matlab® software package for the different phases of the irradiation experiments: exposure, one day holding period (for

*Solutions of stiff differential equations can change on a time scale that is very short compared to the interval of integration, but the solution of interest changes on a much longer time scale.

delayed plating data), exponential and confluent growth. The length of exposure times for the different doses and the different growth phases can be calculated based on information given in Redpath *et al.* (2001) and Mendonca et al. 1989. Data fitting was done with a grid search algorithm that allows searching the parameter space at a global level. Fine tuning was performed with the Nelder-Mead Simplex algorithm (Nelder and Mead 1965). The relative error, $\sum_i \text{abs}\left[\left(\text{TFSC}(i) - f_4(i)\right)/\text{TFSC}(i)\right]$, was used to find best estimates for the free parameters. Here, $\text{TFSC}(i)$ denotes the *i*th measured transformation frequency per surviving cell.

RESULTS

At first, the model without PAM was fitted to the joint data for immediate and delayed plating at control and high doses (fit1, Fig. 3A). This joint fit allowed for more data points. The free parameters of fit1 included a background transformation rate $f_4(0)$ within in the initial state vector: $[1 - f_4(0), 0, 0, 0, 0, f_4(0)]$. This means that prior to irradiation a fraction $f_4(0)$ is already initiated. The values allowed for $f_4(0)$ in the grid search ranged from 10^{-5} to 10^{-4}. In addition, a damping factor ($e^{-\lambda_{decr}D}$) was applied to k_{rs}, k_{rns}, and the cell cycle associated repair (Schöllnberger et al., submitted).

A forward simulation of the full data set for immediate plating with parameter estimates from fit1 as fixed input was performed. This gave the "direct" contribution (Fig. 3B). Then the model with PAM was fitted to the data (fit2, "total" contribution). The data for delayed plating were analyzed analogously (fit3, Fig. 3C). In fit2 and fit3 three free parameters were applied: k_{ap}, the time point for the activation of PAM, denoted as t_{ap_on}, and the time point for the deactivation of PAM, t_{ap_off}. The best estimated values for the free parameters together with the relative errors are given in Table 1. The data for immediate plating show a lower protective effect than the data for delayed plating (Redpath *et al.* 2001). This is reflected in the fact that fit2 exhibits a shallower U-shape than fit3 and a

TABLE 1. Best Estimates, Relative Errors and Variances for Model Fits of the Redpath *et al.* (2001) data.

Fit1	Fit2	Fit3
k_{01sb} = 0.55/day	k_{ap} = 0.11/day	k_{ap} = 0.11/day
k_{01nsb} = 10.22/day	t_{ap_on} = 5.08 days	t_{ap_on} = 9.90 days
k_{01nsr} = 151.42/Gy	t_{ap_off} = 7.30 days	t_{ap_off} = 15.46 days
$f_4(0)$ = 2.63·10^{-5}		
λ_{decr} = 0.08/Gy		
Relative error = 0.550	Relative error = 0.591, σ^2 = 0.092	Relative error = 0.591, σ^2 = 0.070

Note: In fit1 the control and high dose data points at 0.3, 0.5 and 1 Gy for immediate and delayed plating were fitted jointly. The best estimated values from fit1 were used as fixed input in fit2 and fit3. Fit2: immediate plating, fit3: delayed plating. In all fits $k_{mmult} \equiv 1$.

smaller initial drop from 0 to 1 mGy (inserts in Figs. 3B and 3C). The best estimated value for PAM duration ($t_{ap\_off} − t_{ap\_on} = 2.2$ days) in fit2 is accordingly smaller than in fit3 with similar values for k_{ap}.

DISCUSSION AND CONCLUSIONS

The SVM is biologically motivated as recently pointed out (Schöllnberger et al., submitted). It describes an important process in the formation of neoplastic transformation: chromosome aberrations, specifically, translocations and inversions (page 556 in Friedberg 1985). The repair pathways represent DSB repair in quiescent cells (k_{rs} and k_{rns}) and cell cycle associated repair related to mitotic rate constant k_m. Despite its relation to k_m, the cell cycle associated repair does not occur during mitosis but represents a postreplication repair pathway. After the interaction of the two types of DSBs (which forms state 3 cells) the damage is made permanent when state 3 cells divide. Cells may resume cell cycle progression in the presence of unrepaired damage, a process called *adaptation* (Friedberg et al. 2006). In yeast is has been shown that such adaptation enhances survival, but at a price. Chromosome loss and translocations are elevated in the surviving clones (Galgoczy and Toczyski 2001). This is simulated in the SVM in a simplified way by applying a constant probability per cell division that a state 3 cell develops into an unrepairable mutated cell (state 4; refer to *Materials and Methods* section). The concept of unrepairable initiated cells is firmly established (Moolgavkar and Knudson 1981, Trosko et al. 1990). For the simulation of *in vitro* neoplastic transformation, the SVM then describes the clonal expansion of a fraction *F* of the initiated cells that have a decreased gap junctional intercellular communication (Trosko and Ruch 1998). For the fit of the Redpath et al. (2001) data *F* = 1 is used because the CGL1 cells show a lack of density-dependent inhibition of division (Stanbridge and Wilkinson 1978). The conclusions reached in the current study assume that the biological concepts and related model assumptions are valid.

Previous low dose studies with the SVM (Schöllnberger *et al.* 1999, 2002) focused on explaining a form of induced radio-resistance that might be visible in a plateau in the dose-response curve for neoplastic transformation of C3H 10T1/2 cells irradiated with acute doses of X-rays (Miller *et al.* 1979). Another data set applied by Schöllnberger *et al.* (1999) exhibits a plateau for chromosome aberrations induced by acute γ-irradiation of rat hepatocytes (Eckl *et al.* 1993). The plateaus were explained with radiologically inducible DSB repair and radical scavenging. Eckl *et al.* (1993) also pre-irradiated the cells with low doses. That led to reduced detrimental effects of the acute irradiations visible in lower dose-response curves for chromosome aberrations. We explained this more classical adaptive response with elevated background rates for repair and scavenging caused by the 2.5 mGy prime irradiation (Schöllnberger *et al.* 1999).

In another study (Schöllnberger *et al.* 2002) the SVM was fitted to U-shaped data by Azzam (1994). This data set shows a U-shaped dose-response for neoplastic transformation in C3H 10T1/2 cells irradiated with γ-rays (0.1 – 5 Gy) at low dose rate (2.4 mGy/min). Together with another set of data (Azzam *et al.* 1996), this data set was explained by the model with radiologically enhanced repair rates and increased radical scavenging capacities of the irradiated cells (Schöllnberger *et al.* 2002).

The current study investigates whether a U-shaped dose response curve for neoplastic transformation can be explained with bystander-induced apoptosis. This follows earlier studies by Scott et al. (2003) and Scott (2004) and has recently been proposed by Portess et al. (2007). Clearly, the model can be successfully fitted to the data (Fig. 3). Both, the data for immediate and delayed plating can be explained. The SVM solution reflects the time dependence of $N_i(t)$ (i = 0, 1s, 1ns, 2, 3, 4) in the formation of neoplastic transformation. Therefore, it can be used to estimate by data fitting the onset and cessation of PAM in addition to its rate k_{ap}. The current study predicts that in the cell culture experiments for delayed plating of Redpath *et al.* (2001) bystander-induced apoptosis is switched on at approximately 10 days postirradiation and that it ceases around day 15 (fit3, Table 1). This should be tested in an experiment.

The value found for the time span that PAM is activated, $t_{ap\_off} - t_{ap\_on}$, is approximately 5 days (fit3). This relatively long time is reflected in the scientific literature. Jamali and Trott (1996) report a two week induction of apoptosis after a 1 Gy X-irradiation at 0.5 Gy/min. Mendonca *et al.* (1999) showed that after a 7 Gy high dose X-irradiation apoptosis is switched on in CGL1 cells approximately 9 days postirradiation and switched off around day 15 to 18. The best estimated values of fit3 reflect these results. In another study only one free parameter, k_{ap}, was used (Schöllnberger et al., submitted). There, it was assumed that PAM is activated immediately after the exposure ended and that it is deactivated at the end of exponential growth, i.e. $t_{ap\_off} \equiv$ 11 days + ET. The best estimated value for k_{ap} was 0.054/day for delayed plating with a relative error of 0.642 (Schöllnberger et al., submitted). In fit3 k_{ap} = 0.11/day with an approximate 5 day time of PAM induction. This shows that k_{ap} and the time of PAM induction are inversely related to each other: a shorter time of PAM induction can compensate for a larger value of k_{ap} and vice versa. When two free parameters, k_{ap} and t_{ap_off}, were applied, the best estimated values were 0.025/day and 23.67 days, respectively (Schöllnberger et al., submitted). That confirms the inverse relation of k_{ap} and PAM induction. It is worth to mention that in fit2 and fit3 very large 95% confidence intervals for the free parameters were found.

The question emerges whether the presented model fits with three free parameters represent descriptions of the data that are statistically significantly better than those fits with only one or two free parameters. The

F-test can be used to decide this. This test allows to decide with a chosen confidence whether the variances of two samples from different populations are statistically significantly different. One calculates $F = \sigma_1^2/\sigma_2^2$ where σ_i^2 is the variance of the ith sample (here: model fit). For the model fits presented here, the variance is $\sigma^2 = \sum_{i=1}^{9}\left((\text{TFSC}(i) - f_4(i))/\text{TFSC}(i)\right)^2$. Here, $f_4(i)$ is the model prediction for the ith data point (refer to eq. (7)). The calculated F-value is then compared to the corresponding entry on a table of F-test critical values at a significance level of $\alpha = 0.05$ for m and n degrees of freedom (dof), and dof = number of data points – number of free parameters – 1. For the earlier fit of the data for delayed plating with k_{ap} as free parameter, $m = 7$ and $\sigma^2 = 0.074$ (Schöllnberger et al., submitted). For fit3 with its 3 free parameters, $n = 5$ and $\sigma^2 = 0.070$ (Table 1). One gets F = 0.074/0.070 = 1.06 which is smaller than the tabulated value of 4.876 at $\alpha = 0.05$ for $m = 7$ and $n = 5$. Therefore, it can be said that with a probability of 0.95 the two variances are not significantly different. Fit3 is at the 5% significance level not better than the fit with one free parameter. An analogous result was found with respect to the fit that had two free parameters, k_{ap} and t_{ap_off}. This means that the data at hand cannot be used to prove that the model with three free parameters is better than the model with one or two free parameters. However, we still believe that the best estimates found for k_{ap} and t_{ap_off} in fit3 are interesting especially with respect to the fact that they are reflected in the scientific literature as discussed above. A higher number of data points would be necessary for larger values for m and n and consequently smaller tabulated F-test values so that the different model fits are statistically discernible.

The presented model for the protective apoptosis-mediated bystander effect bears similarities to the approach by (Scott 2004) who also applied PAM to fit the Redpath *et al.* (2001) data and another U-shaped data set for mutation frequencies (Scott *et al.* 2004). Both groups currently model PAM as dose-rate independent. A dose rate dependence has been found for apoptosis induction (Boreham *et al.* 2000) but not for the dose rate of 3.3 mGy/min used by Redpath *et al.* (2001).

While the current model explains the U-shaped dose-response curve in the Redpath et al. (2001) data with an apoptosis-mediated protective bystander effect, other mechanisms such as upregulation of DNA repair and radical scavenging and cell killing of a transformation sensitive sub-component of the overall cell population could also contribute to the observed protective effects in a dose-dependent way (Azzam et al. 1996, Redpath et al. 2001, Pant et al. 2003, Ko et al. 2004). The data by Redpath et al. (2001) and Azzam et al. (1996) are not in contradiction to other *in vitro* data for neoplastic transformation that do not show a U-shaped dose response at low doses. This has to do with the different dose rates applied, different experimental protocols including delayed plating and the fact

that many of these other studies have a lowest dose that is too high to reveal any possible protective effects. For example, the lowest dose in the X-ray data by Mill et al. (1998) is at 250 mGy while Redpath et al. (2003) and Ko et al. (2004) found the transition between protection and detriment from X-ray exposures at lower doses. This has been discussed in more detail by Schöllnberger et al. (2002) and Schöllnberger et al. (submitted).

While we have stated that it is not yet decided whether at low doses bystander effects are predominately detrimental or protective with respect to cancer induction in humans, we do, however, tend to agree with other researchers who have stated that bystander effects are positive cellular manifestations of multicellular damage responses and that they are evidence of the extracellular signaling that results from such multicellular programs that attempt to re-establish homeostasis and eliminate abnormal cells (Barcellos-Hoff and Brooks 2001, Barcellos-Hoff and Costes 2006). Mothersill and Seymour (2006) argue that cell communication via signaling pathways is coordinating the radiation response at low doses and that bystander effects are beneficial at some level of organization that supersedes the individual cell. They also pose the fascinating suggestion that genomic instability may represent part of the mechanism by which adaptation to altered environmental conditions is achieved at the population level (Mothersill and Seymour 2006).

Summarizing, it can be said:

- A protective apoptosis-mediated bystander effect could at least in part be responsible for protective effects of low doses of γ-radiation.
- Our findings for the onset and cessation of bystander-induced apoptosis after low doses of γ-radiation are in accordance to reported experimental results for higher doses of low-LET radiation.
- New experiments are needed to investigate the time dependence of apoptosis induction and cessation at low doses < 200 mGy.
- Future modeling studies should include other low dose data of Dr. Redpath's group published in the recent years.
- The PAM process should be generalized so that possible dose-rate dependencies and other biological details of its induction can be described.
- The importance of adaptive responses with respect to a reduction of transformation and mutation frequencies *below* the background neoplastic transformation and mutation frequencies after a *single* low dose irradiation is emphasized.
- The current predominant notion of bystander effects as detrimental needs to be extended to also include its protective features.

REFERENCES

Azzam EI. 1994. Adaptive responses to ionizing radiation in normal human skin fibroblasts. Dissertation, University of Ottawa, Ottawa

Azzam EI, de Toledo SM, Raaphorst GP, and Mitchel REJ. 1996. Low-dose ionizing radiation decreases the frequency of neoplastic transformation to a level below the spontaneous rate in C3H 10T1/2 cells. Radiat Res 146(4): 369-373

Barcellos-Hoff MH and Brooks AL. 2001. Extracellular signaling through the microenvironment: a hypothesis relating carcinogenesis, bystander effects, and genomic instability. Radiat Res 156(5 Pt 2): 618-627

Barcellos-Hoff MH and Costes SV. 2006. A systems biology approach to multicellular and multi-generational radiation responses. Mutat Res 597(1-2): 32-38

Bauer G. 1996. Elimination of transformed cells by normal cells: a novel concept for the control of carcinogenesis. Histol Histopathol 11(1): 237-255

Bauer G. 2000. Reactive oxygen and nitrogen species: efficient, selective, and interactive signals during intercellular induction of apoptosis. Anticancer Res 20(6B): 4115-4139

Belyakov OV, Folkard M, Mothersill C, Prise KM, and Michael BD. 2002. Bystander-induced apoptosis and premature differentiation in primary urothelial explants after charged particle microbeam irradiation. Radiat Prot Dosim 99(1-4): 249-251

Belyakov OV, Folkard M, Mothersill C, Prise KM, and Michael BD. 2003. A proliferation-dependent bystander effect in primary porcine and human urothelial explants in response to targeted irradiation. Brit J Cancer 88(5): 767-774

Belyakov OV, Mitchell SA, Parikh D, Randers-Pehrson G, Marino SA, Amundson SA, Geard CR, and Brenner DJ. 2005. Biological effects in unirradiated human tissue induced by radiation damage up to 1 mm away. Proc Natl Acad Sci USA 102(40): 14203-14208

Boreham DR, Dolling JA, Maves SR, Siwarungsun N, and Mitchel REJ. 2000. Dose-rate effects for apoptosis and micronucleus formation in gamma-irradiated human lymphocytes. Radiat Res 153(5 Pt 1): 579-586

Brenner DJ, Little JB, and Sachs RK. 2001. The bystander effect in radiation oncogenesis: II. A quantitative model. Radiat Res 155(3): 402-408

Brooks AL. 2005. Paradigm shifts in radiation biology: their impact on intervention for radiation-induced disease. Radiat Res 164(4 Pt 2): 454-461

Broome EJ, Brown DL, and Mitchel REJ. 1999. Adaptation of human fibroblasts to radiation alters biases in DNA repair at the chromosomal level. Int J Radiat Biol 75(6): 681-690

Chaudhry MA. 2006. Bystander effect: biological endpoints and microarray analysis. Mutat Res 597(1-2): 98-112

Crawford-Brown DJ and Hofmann W. 1990. A generalized state-vector model for radiation-induced cellular transformation. Int J Radiat Biol 57(2): 407-423

Dormann S, Schwieger A, Hanusch J, Haufel T, Engelmann I, and Bauer G. 1999. Intercellular induction of apoptosis through modulation of endogenous survival factor concentration: a review. Anticancer Res 19(1A): 87-103

Dormann S and Bauer G. 1998. TGF-beta and FGF trigger intercellular induction of apoptosis: analogous activity on non-transformed but differential activity on transformed cells. Int J Oncol 13(6): 1247-1252

Eckert S and Bauer G. 1998. TGF-beta isoforms and fibroblast growth factor exhibit analogous indirect antioncogenic activity through triggering of intercellular induction of apoptosis. Anticancer Res 18(1A): 45-52

Eckl PM, Karpf ABC, Stöß W, Knasmüller S, and Schulte-Hermann R. 1993. Comparative investiga-tion on genotoxic effects induced by gamma-radiation and Diesel exhaust in primary cultures of adult rat hepatocytes. Proceedings of the IAEA/UNEP Seminar for Africa, Europe, the Middle East and the Mediterranean on Radiobiologial Techniques in the Comparative Estimation of Carcinogenic Induction by Chemical Pollutants and Low-dose Radiation, Nairobi, IAEA-SR-184-10

Feinendegen LE and Pollycove M. 2001. Biologic responses to low doses of ionizing radiation: detri-ment versus hormesis. Part 1. Dose responses of cells and tissues. J Nucl Med 42(7): 17N-27N

Fleishman L, Crawford-Brown DJ, and Hofmann W. Application of a generalized state-vector model for radiation-induced cellular transformation to *in vitro* irradiation of cells by acute doses of X-rays. Submitted

Friedberg EC. 1985. DNA Repair. WH Freeman, New York

Friedberg EC, Walker GC, Siede W, Wood RD, Schultz RA, and Ellenberger T. 2006. DNA repair and mutagenesis. ASM Press. Washington, DC

Galgoczy DJ and Toczyski DP. 2001. Checkpoint adaptation precedes spontaneous and damage-induced genomic instability in yeast. Mol Cell Biol 21(5): 1710-1718

Hall EJ and Hei TK. 1985. Oncogenic transformation with radiation and chemicals. Int J Radiat Biol Relat Stud Phys Chem Med 48(1): 1-18

Heigold S, Sers C, Bechtel W, Ivanovas B, Schafer R, and Bauer G. 2002. Nitric oxide mediates apop-tosis induction selectively in transformed fibroblasts compared to nontransformed fibroblasts. Carcinogenesis 23(6): 929-941

Höfler P, Wehrle I, and Bauer G. 1993. TGF-beta induces an inhibitory effect of normal cells direct-ed against transformed cells. Int J Cancer 54(1): 125-130

Iyer R and Lehnert BE. 2002. Alpha-particle-induced increases in the radioresistance of normal human bystander cells. Radiat Res 157(1): 3-7

Jamali M and Trott KR. 1996. Persistent increase in the rates of apoptosis and dicentric chromosomes in surviving V79 cells after X-irradiation. Int J Radiat Biol 70(6): 705-709

Jürgensmeier JM, Schmitt CP, Viesel E, Höfler P, and Bauer G. 1994a. TGF-ß-treated normal fibro-blasts eliminate transformed fibroblasts by induction of apoptosis. Cancer Res 54(2): 393-398

Jürgensmeier JM, Höfler P, and Bauer G. 1994b. TGF-ß-induced elimination of transformed fibro-blasts by normal cells: independence of cell-to-cell contact and dependence on ROS. Int J Oncol 5: 525-531

Ko SJ, Liao XY, Molloi S, Elmore E, and Redpath JL. 2004. Neoplastic transformation *in vitro* after exposure to low doses of mammographic-energy X rays: quantitative and mechanistic aspects. Radiat Res 162(6): 646-654

Konopacka M and Rzeszowska-Wolny J. 2006. The bystander effect-induced formation of micronu-cleated cells is inhibited by antioxidants, but the parallel induction of apoptosis and loss of via-bility are not affected. Mutat Res 593(1-2): 32-38

Langer C, Jürgensmeier JM, and Bauer G. 1996. Reactive oxygen species act at both TGF-β-depend-ent and -independent steps during induction of apoptosis of transformed cells by normal cells. Exp Cell Res 222(1): 117-124

Little JB. 1985. Cellular mechanisms of oncogenic transformation *in vitro*. IARC Sci Publ 67: 9-29

Little MP. 1995. Are two mutations sufficient to cause cancer? Some generalizations of the two-muta-tion model of carcinogenesis of Moolgavkar, Venzon, and Knudson, and of the multistage model of Armitage and Doll. Biometrics 51(4): 1278-1291

Luebeck EG, Heidenreich WF, Hazelton WD, Paretzke HG, and Moolgavkar SH. 1999. Biologically based analysis of the data for the Colorado uranium miners cohort: age, dose and dose-rate effects. Radiat Res 152(4): 339-351

Lyng FM, Seymour CB, and Mothersill C. 2000. Production of a signal by irradiated cells which leads to a response in unirradiated cells characteristic of initiation of apoptosis. Br J Cancer 83(9): 1223-1230

Lyng FM, Seymour CB, and Mothersill C. 2002a. Early events in the apoptotic cascade initiated in cells treated with medium from the progeny of irradiated cells. Radiat Prot Dosim 99(1-4): 169-172

Lyng FM, Seymour CB, and Mothersill C. 2002b. Initiation of apoptosis in cells exposed to medium from the progeny of irradiated cells: a possible mechanism for bystander-induced genomic instability? Radiat Res 157(4): 365-370

Lyng FM, Maguire P, Kilmurray N, Mothersill C, Shao C, Folkard M, and Prise KM. 2006. Apoptosis is initiated in human keratinocytes exposed to signalling factors from microbeam irradiated cells. Int J Radiat Biol 82(6): 393-399

Maguire P, Mothersill C, Seymour C, and Lyng FM. 2005. Medium from irradiated cells induces dose-dependent mitochondrial changes and BCL2 responses in unirradiated human keratinocytes. Radiat Res 163(4): 384-390

Mebust MR, Crawford-Brown DJ, Hofmann W, and Schöllnberger H. 2002. Testing extrapolation of a biologically-based exposure-response model from *in vitro* to *in vivo* to human epidemiological conditions. Reg Toxicol Pharmacol 35(1): 72-79

Mendonca MS, Kurohara W, Antoniono R, and Redpath JL. 1989. Plating efficiency as function of time postirradiation: evidence for the delayed expression of lethal mutations. Radiat Res 119(2): 387-393

Mendonca MS, Howard KL, Farrington DL, Desmond LA, Temples TM, Mayhugh BM, Pink JJ, and Boothman DA. 1999. Delayed apoptotic responses associated with radiation-induced neoplastic transformation of human hybrid cells. Cancer Res 59(16): 3972-3979

Mill AJ, D. Frankenberg, D. Bettega, L. Hieber, A. Saran, L. A. Allen, P. Calzolari, M. Frankenberg-Schwager, M. M. Lehane, and L. Tallone, 1998. Transformation of C3H 10T1/2 cells by low doses of ionising radiation: a collaborative study by six European laboratories strongly supporting a linear dose-response relationship. J Radiol Prot 18(2): 79-100

Miller RC, Hall EJ, and Rossi HH. 1979. Oncogenic transformation of mammalian cells *in-vitro* with split doses of X-rays. Proc Natl Acad Sci USA 76(11): 5755-5758

Miller RC, Marino SA, Brenner DJ, Martin SG, Richards M, Randers-Pehrson G, and Hall EJ. 1995. The biological effectiveness of radon-progeny alpha particles. II. Oncogenic transformation as a function of linear energy transfer. Radiat Res 142(1): 54-60

Mitchel REJ, Jackson JS, McCann RA, and Boreham DR. 1999. The adaptive response modifies latency for radiation-induced myeloid leukemia in CBA/H mice. Radiat Res 152(3): 273-279

Mitchel REJ, Dolling J-A, Misonoh J, and Boreham DR. 2002. Influence of prior exposure to low dose adapting radiation on radiation induced teratogenic effects in fetal mice with varying Trp53 function. Radiat Res 158(4): 458-463

Mitchel REJ, Jackson JS, Morrison DP, and Carlisle SM. 2003. Low doses of radiation increase the latency of spontaneous lymphomas and spinal osteosarcomas in cancer prone, radiation sensitive *Trp53* heterozygous mice. Radiat Res 159(3): 320-327

Mitchel REJ, Jackson JS, and Carlisle SM. 2004. Upper dose thresholds for radiation-induced adaptive response against cancer in high-dose-exposed, cancer-prone, radiation-sensitive Trp53 heterozygous mice. Radiat Res 162(1): 20-30

Mitchel REJ. 2006. Low doses of radiation are protective *in vitro* and *in vivo*: evolutionary origins. Dose Response 4(2): 75-90

Mitchel REJ. 2007. Low doses of radiation reduce risks *in vivo*. Dose Response 5(1): 1-10

Moolgavkar SH and Knudson AG Jr. 1981. Mutation and cancer: a model for human carcinogenesis. J Natl Cancer Inst 66(6): 1037-1052

Morgan WF. 2003a. Non-targeted and delayed effects of exposure to ionizing radiation: I. Radiation-induced genomic instability and bystander effects *in vitro*. Radiat Res 159(5): 567-580

Morgan WF. 2003b. Non-targeted and delayed effects of exposure to ionizing radiation: II. Radiation-induced genomic instability and bystander effects *in vivo*, clastogenic factors and transgenerational effects. Radiat Res 159(5): 581-596

Mothersill C and Seymour C. 1997. Medium from irradiated human epithelial cells but not human fibroblasts reduces the clonogenic survival of unirradiated cells. Int J Radiat Biol 71(4): 421-427

Mothersill C and Seymour C. 2005. Radiation-induced bystander effects: are they good, bad or both? Med Confl Surviv 21(2): 101-110

Mothersill C and Seymour CB. 2006. Actions of radiation on living cells in the "post-bystander" era. EXS 96: 159-177

Nagasawa H and Little JB. 1999. Unexpected sensitivity to the induction of mutations by very low doses of alpha-particle radiation: evidence for a bystander effect. Radiat Res 152(5): 552-557

Nagasawa H and Little JB. 2002. Bystander effect for chromosomal aberrations induced in wild- type and repair deficient CHO cells by low fluences of alpha particles. Mutat Res 508(1-2): 121-129

NCRP. Evaluation of the linear-nonthreshold dose-response model for ionizing radiation, 2001. NCRP Report 136, Bethesda, MD

Nelder JA and Mead R. 1965. A simplex method for function minimization. Computer J 7: 308-313

Nikjoo H and Khvostunov IK. 2003. Biophysical model of the radiation-induced bystander effect. Int J Radiat Biol 79(1): 43-52

Pant MC, Liao XY, Lu Q, Molloi S, Elmore E, and Redpath JL. 2003. Mechanisms of suppression of neoplastic transformation *in vitro* by low doses of low LET radiation. Carcinogenesis 24(12): 1961-1965

Portess DI, Bauer G, Hill MA, and O'Neill P. 2007. Low dose irradiation of non-transformed cells stimulates the selective removal of pre-cancerous cells via intercellular induction of apoptosis. Cancer Res 67(3): 1246-1253

Prise KM, Schettino G, Folkard M, and Held KD. 2005. New insights on cell death from radiation exposure. Lancet Oncol 6(7): 520-528

Redpath LJ and Antoniono RJ. 1998. Induction of an adaptive response against spontaneous neoplastic transformation *in vitro* by low-dose gamma radiation. Radiat Res 149(5): 517-520

Redpath JL, Liang D, Taylor TH, Christie C, and Elmore E. 2001. The shape of the dose response curve for radiation-induced neoplastic transformation *in vitro*: evidence for an adaptive response against neoplastic transformation at low doses of low-LET radiation. Radiat Res 156(6): 700-707

Redpath JL, Lu Q, Lao X, Molloi S, and Elmore E. 2003. Low doses of diagnostic energy X-rays protect against neoplastic transformation *in vitro*. Int J Radiat Biol 79(4): 235-240

Sak A and Stuschke M. 1998. Repair of ionizing radiation induced DNA double-strand breaks (dsb) at the c-myc locus in comparison to the overall genome. Int J Radiat Biol 73(1): 35-43

Sawant SG, Randers-Pehrson G, Geard CR, Brenner DJ and Hall EJ. 2001. The bystander effect in radiation oncogenesis. I. Transformation in C3H 10T1/2 cells *in vitro* can be initiated in the unirradiated neighbors of irradiated cells. Radiat Res 155(3): 397-401

Schöllnberger H, Kotecki MR, Crawford-Brown DJ, Hofmann W, and Eckl PM. 1999. Adaptive response and dose-response plateaus for initiation in a state-vector model of carcinogenesis. Int J Radiat Biol 75(3): 351-364

Schöllnberger H, Mitchel REJ, Azzam EI, Crawford-Brown DJ, and Hofmann W. 2002. Explanation of protective effects of low doses of γ-radiation with a mechanistic radiobiological model. Int J Radiat Biol 78(12): 1159-1173

Schöllnberger H, Stewart RD, Mitchel REJ, and Hofmann W. 2004. An examination of radiation hormesis mechanisms using a multi-stage carcinogenesis model. Nonlin Biol Toxicol Med 2(4): 317-352

Schöllnberger H, Stewart RD, and Mitchel REJ. 2005. Low-LET-induced radioprotective mechanisms within a stochastic two-stage cancer model. Dose-Response 3(4): 508-518

Schöllnberger H, Mitchel REJ, Crawford-Brown DJ, and Hofmann W. 2006. A model for the induction of chromosome aberrations through direct and bystander mechanisms. Radiat Prot Dosim 122(1-4): 275-281

Schöllnberger H, Mitchel REJ, Redpath JL, Crawford-Brown DJ, and Hofmann W. Detrimental and protective bystander effects: a model approach. Radiat Res, *Submitted*

Scott BR, Walker DM, Tesfaigzi Y, Schöllnberger H, and Walker V. 2003. Mechanistic basis for nonlinear dose-response relationships for low-dose radiation-induced stochastic effects. Nonlin Biol Toxicol Med 1(1): 93-122

Scott BR, Walker DM, and Walker VE. 2004. Low-Dose Radiation and Genotoxic Chemicals Can Protect Against Stochastic Biological Effects. Nonlin Biol Tox Med 2: 185-211

Scott BR. 2004. A biological-based model that links genomic instability, bystander effects, and adaptive response. Mutat Res 568(1): 129-143

Stanbridge EJ and Wilkinson J. 1978. Analysis of malignancy in human cells: malignant and transformed phenotypes are under separate genetic control. Proc Natl Acad Sci USA 75(3): 1466-1469

Trosko JE, Chang CC, and Madhukar BV. 1990. Modulation of intercellular communication during radiation and chemical carcinogenesis. Radiat Res 123(3): 241-251

Trosko JE and Ruch RJ. 1998. Cell-cell communication in carcinogenesis. Front Biosci 3(3): d208-236

Zhou H, Randers-Pehrson G, Waldren CA, Vannais D, Hall EJ, and Hei TK. 2000. Induction of a bystander mutagenic effect of alpha particles in mammalian cells. Proc Natl Acad Sci USA 97(5): 2099-2104